

# Mixture of Inference Networks for VAE-based Audio-visual Speech Enhancement

Mostafa Sadeghi and Xavier Alameda-Pineda, *Senior Member, IEEE*

**Abstract**—In this paper, we are interested in unsupervised (unknown noise) speech enhancement using latent variable generative models. We propose to learn a generative model for clean speech spectrogram based on a variational autoencoder (VAE) where a mixture of audio and visual networks is used to infer the posterior of the latent variables. This is motivated by the fact that visual data, i.e. lips images of the speaker, provide helpful and complementary information about speech. As such, they can help train a richer inference network, where the audio and visual information are fused. Moreover, during speech enhancement, visual data are used to initialize the latent variables, thus providing a more robust initialization than using the noisy speech spectrogram. A variational inference approach is derived to train the proposed VAE. Thanks to the novel inference procedure and the robust initialization, the proposed audio-visual VAE exhibits superior performance on speech enhancement than using the standard audio-only counterpart.

**Index Terms**—Audio-visual speech enhancement, generative models, variational auto-encoder, mixture model

## I. INTRODUCTION

**S**PEECH enhancement, or removing background noise from noisy speech [1], [2], is a classic yet very important problem in signal processing and machine learning. Traditional solutions to this problem are based on spectral subtraction [3] and Wiener filtering [4], targeting noise and/or speech power spectral density (PSD) estimation in the short-time Fourier transform (STFT) domain. The recent impressive performance of deep neural networks (DNNs) in computer vision and machine learning has paved the way to revisit the speech enhancement problem. DNNs have been widely utilized in this regard, where a neural network is trained to map a noisy speech spectrogram to its clean version, or to a time frequency (TF) mask [5]–[7]. This is usually done in a supervised way, using a huge dataset of noise and clean speech signals for training. As such, the performance of a supervised speech enhancement technique often degrades when dealing with an unknown type of noise.

Unsupervised techniques offer another procedure for speech enhancement that does not use noise signals for training. A popular unsupervised method is based on nonnegative matrix factorization (NMF) [8]–[10] for modeling the PSD of speech signals [11], which decomposes PSD as a product of two non-negative low-rank matrices (a dictionary of basis spectra and the corresponding activations). An NMF-based speech enhancement method consists of first learning a set of basis

spectra for clean speech spectrograms at training phase, prior to speech enhancement [9], [12], [13]. Then, by decomposing the noisy spectrogram as the sum of clean speech and noise spectrograms, the corresponding clean speech activations as well as the NMF parameters of noise are estimated. While being computationally efficient, this modeling and enhancement framework cannot properly explain complicated structure of speech spectrogram due to the limited representational power dictated by the two low-rank matrices. A deep autoencoder (DAE) has been employed in [14] to model clean speech and noise spectrograms. A DAE is pre-trained for clean speech spectrograms, whereas an extra DAE for noise spectrogram is trained at the enhancement stage using the noisy spectrogram. The corresponding inference problem is under-determined, and the authors proposed to constrain the unknown speech using a pre-trained NMF model. As such, this DAE-based method might encounter the same shortcomings as those of the NMF-based speech enhancement [15].

Deep latent variable models offer a more sophisticated and efficient modeling framework than NMF and DAE, gaining much interest over the past few years [15]–[20]. The first and main step is to train a generative model for clean speech spectrogram using a variational auto-encoder (VAE) [21], [22]. VAE provides an efficient way to estimate the parameters of a non-linear generative model, also called the decoder. This is done by approximating the intractable posterior distribution of the latent variables using a Gaussian distribution parametrized by a neural network, called the inference (encoder) network. The encoder and decoder are jointly trained to maximize a variational lower bound on the marginal data log-likelihood. At test time, the trained generative model is combined with a noise model, e.g. NMF. The unknown noise parameters and clean speech are then estimated from the observed noisy speech. Being independent of the noise type at training, these methods show better generalization than the supervised approaches [15], [16].

Motivated by the fact that the visual information, when associated with audio information, often helps improve the quality of speech enhancement [23]–[25], an audio-visual latent variable generative model has recently been proposed in [26]. Within this model, the visual features corresponding to the lips region of the speaker are also fed to the encoder and decoder networks of the VAE. The effectiveness and superior performance of the audio-visual VAE (AV-VAE) compared to the audio-only VAE (A-VAE), as well as the supervised deep learning based method of [25] has been experimentally verified in [26]. To deal with noisy visual data at test time, e.g. non-frontal or occluded lips images, a robust method has

Xavier Alameda-Pineda acknowledges ANR and the IDEX for funding the ML3RI project.

The authors are with the Perception team at Inria Grenoble Rhône-Alpes, France.

been proposed in [27], where during speech enhancement, a mixture of trained A-VAE and AV-VAE is used as the clean speech model. Because of that, the deteriorating effects associated with missing/noisy visual information are avoided as the algorithm switches from AV-VAE to A-VAE in these cases [27]. Besides AV-VAE, a video-only VAE (V-VAE) has also been introduced in [26], where the posterior parameters of the latent variables, that is, the encoder parameters, are trained using only visual information. As such, the latent variables governing the generative process of clean speech spectrogram are inferred from visual data only. V-VAE has been shown to yield much better speech enhancement performance than A-VAE when the noise level is high [26].

In the speech enhancement phase, because of the non-linear generative model, the posterior of the latent variables does not admit a closed-form expression. Two approaches are often used to get around this problem. The first solution is based on the Markov Chain Monte Carlo (MCMC) method [28], in which a sampling technique, e.g. the Metropolis-Hastings algorithm [28], is used to sample from the posterior [15], [16]. The obtained samples are then used to approximate the expectations using the Monte-Carlo average. The second approach makes use of optimization techniques to find the maximum a posteriori estimation of the latent variables [20]. In either case, the initialization plays an important role, as the associated problems are highly non-convex. In practice, the trained encoder is used to initialize the latent variables by giving the noisy speech spectrogram as the input and taking the posterior mean at the output. This can partly explain why V-VAE performs better than A-VAE at high noise levels. In fact, the latent variable initialization in V-VAE is based on visual features, whereas in A-VAE, it is based on the noisy speech. As a result, V-VAE provides a better initialization, because it uses noise-free data (visual features) [26].

The original contribution of this paper is to optimally exploit the complementarity of A-VAE and V-VAE, without systematic recourse to simultaneously using audio and visual features, i.e. via simple concatenation (tight fusion) as done in AV-VAE. Indeed, we aim to bridge the performance gap between A-VAE and V-VAE by designing a mixture of audio and visual inference (encoder) networks, called mixture of inference networks VAE (MIN-VAE). The inputs to audio and visual encoders are speech spectrogram frames and the corresponding visual features, respectively, thus training MIN-VAE to select the best combination of the the audio and video information. A variational inference approach is proposed to train the mixture of the two encoders jointly with a shared decoder (generative) network. This way, the decoder reconstructs the input audio data using the optimal combination of the audio and visual latent samples. At test time, the latent variables are initialized using the visual encoder, thus providing a robust initialization. Our experiments show that MIN-VAE yields much better performance than previous methods, i.e. A-VAE, V-VAE, and AV-VAE.

It should be noted that there are some fundamental differences between our proposed MIN-VAE and the mixture model introduced in [27]. While the purpose of our work is to combine an A-VAE with a V-VAE to take advantage of both

the models, the work in [27] addresses robust audio-visual speech enhancement. We achieve our goal by proposing a VAE architecture with a single decoder but a mixture of audio- and video-based encoders. A new inference method is also derived to train the proposed VAE. In [27], the robustness is achieved by considering a mixture of an A-VAE's decoder and an AV-VAE's decoder at test phase. Both the decoders have been trained separately (using standard A-VAE and AV-VAE), and no particular VAE architecture is trained.

The rest of the paper is organized as follows. In Section II, we review clean speech modeling using already proposed VAE architectures. Next, Section III introduces our proposed MIN-VAE modeling and the associated speech enhancement strategy. Experimental results are then presented in Section IV.

## II. VAE-BASED SPEECH MODELING

### A. Audio-only VAE

Let  $\mathbf{s}_n \in \mathbb{C}^F$  denote the vector of speech STFT coefficients at time frame  $n$ , for  $n \in \{0, \dots, N-1\}$ , which is assumed to be generated according to the following latent variable model [15], [16]:

$$\mathbf{s}_n | \mathbf{z}_n \sim \mathcal{N}_c(\mathbf{0}, \text{diag}(\boldsymbol{\sigma}_s(\mathbf{z}_n))), \quad (1)$$

$$\mathbf{z}_n \sim \mathcal{N}(\mathbf{0}, \mathbf{I}), \quad (2)$$

where  $\mathbf{z}_n \in \mathbb{R}^L$ , with  $L \ll F$ , is a latent random variable describing a speech generative process,  $\mathcal{N}_c(\mathbf{0}, \boldsymbol{\Sigma})$  denotes a zero-mean complex proper Gaussian distribution with covariance matrix  $\boldsymbol{\Sigma}$ , and  $\mathcal{N}(\mathbf{0}, \mathbf{I})$  stands for a zero-mean Gaussian distribution with identity covariance matrix. Moreover,  $\boldsymbol{\sigma}_s(\cdot) : \mathbb{R}^L \mapsto \mathbb{R}_+^F$  is modeled with a neural network parameterized by  $\boldsymbol{\theta}$ , which is called the *decoder*.

In order to estimate the set of parameters,  $\boldsymbol{\theta}$ , using maximum likelihood, one needs to compute the posterior  $p(\mathbf{z}_n | \mathbf{s}_n)$ , which is computationally intractable due to the non-linear likelihood (1). The VAE formalism proposes the use of a tractable variational approximation to  $p(\mathbf{z}_n | \mathbf{s}_n)$  parametrized by a neural network, called the *inference (encoder) network* [22]. This variational distribution writes:

$$q(\mathbf{z}_n | \mathbf{s}_n; \boldsymbol{\phi}_a) = \mathcal{N}(\boldsymbol{\mu}_z^a(\mathbf{s}_n), \text{diag}(\boldsymbol{\sigma}_z^a(\mathbf{s}_n))), \quad (3)$$

where,  $\boldsymbol{\mu}_z^a(\cdot) : \mathbb{R}_+^F \mapsto \mathbb{R}^L$  and  $\boldsymbol{\sigma}_z^a(\cdot) : \mathbb{R}_+^F \mapsto \mathbb{R}_+^L$  are neural networks, with parameters denoted  $\boldsymbol{\phi}_a$ , taking  $\tilde{\mathbf{s}}_n \triangleq (|s_{0n}|^2 \dots |s_{F-1n}|^2)^\top$  as input. Given a sequence of STFT speech time frames  $\mathbf{s} = \{\mathbf{s}_n\}_{n=0}^{N_{tr}-1}$  as training data, with  $\mathbf{z} = \{\mathbf{z}_n\}_{n=0}^{N_{tr}-1}$  being the associated latent variables, the parameters  $\{\boldsymbol{\theta}, \boldsymbol{\phi}_a\}$  are then estimated by maximizing a lower bound on the data log-likelihood  $\log p(\mathbf{s}; \boldsymbol{\theta})$ . Note that,

$$\begin{aligned} \log p(\mathbf{s}; \boldsymbol{\theta}) &= \log \int p(\mathbf{s} | \mathbf{z}; \boldsymbol{\theta}) p(\mathbf{z}) d\mathbf{z} \\ &\geq \mathbb{E}_{q(\mathbf{z} | \mathbf{s}; \boldsymbol{\phi}_a)} \left[ \log \frac{p(\mathbf{s} | \mathbf{z}; \boldsymbol{\theta}) p(\mathbf{z})}{q(\mathbf{z} | \mathbf{s}; \boldsymbol{\phi}_a)} \right] \triangleq \mathcal{L}(\boldsymbol{\theta}, \boldsymbol{\phi}_a) \end{aligned} \quad (4)$$

where, the Jensen's inequality has been used, as it is classically done, see [22]. The function  $\mathcal{L}(\boldsymbol{\theta}, \boldsymbol{\phi}_a)$  is called the evidence

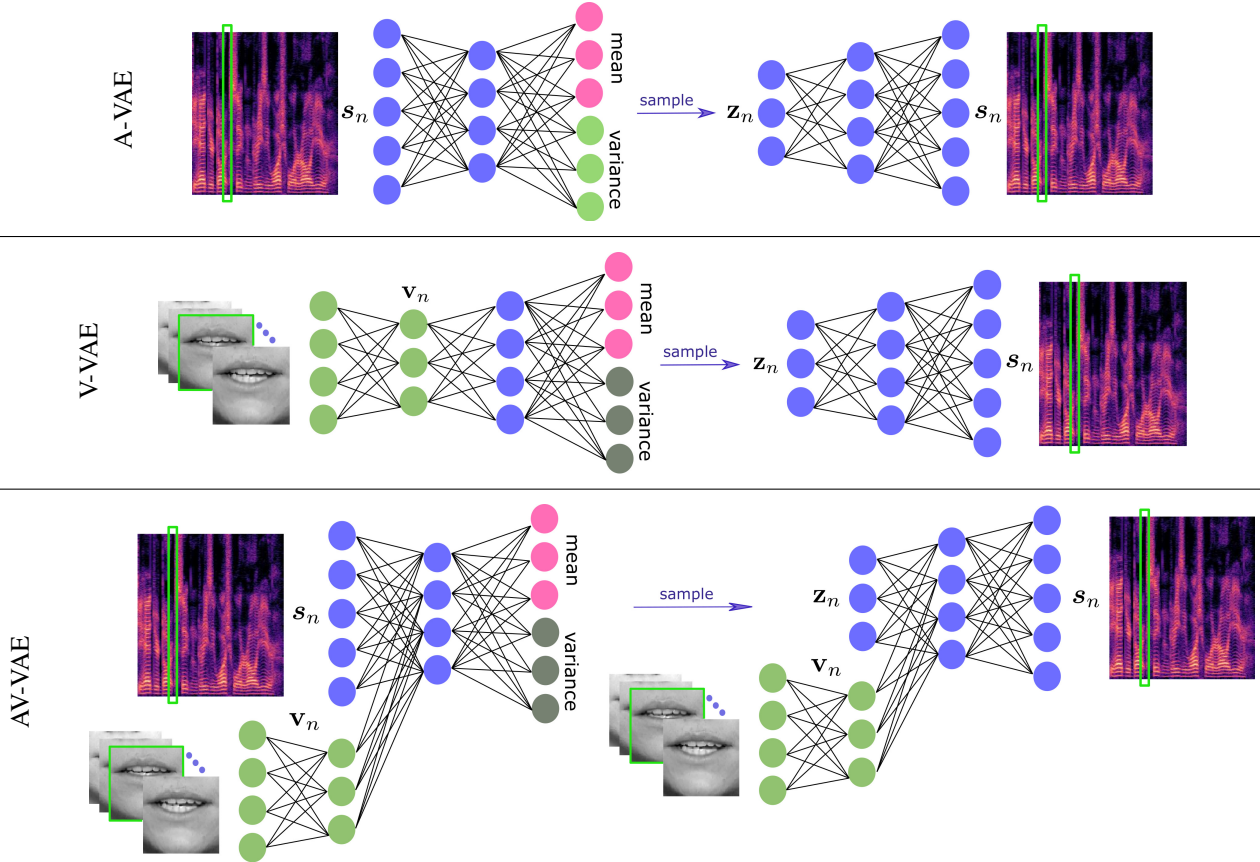


Fig. 1: Architectures for (top) the Audio-only VAE (A-VAE) proposed in [16], (middle) the Video-only VAE (V-VAE) proposed in [26] and (bottom) the Audio-Visual VAE (AV-VAE) proposed in [26].

lower bound (ELBO) [22], because it provides a lower bound on  $\log p(\mathbf{s}; \boldsymbol{\theta})$ . The ELBO can be decomposed as:

$$\mathcal{L}(\boldsymbol{\theta}, \phi_a) = \mathbb{E}_{q(\mathbf{z}|\mathbf{s}; \phi_a)} \left[ \ln p(\mathbf{s}|\mathbf{z}; \boldsymbol{\theta}) \right] - \mathcal{D}_{KL}(q(\mathbf{z}|\mathbf{s}; \phi_a) \| p(\mathbf{z})), \quad (5)$$

where,  $\mathcal{D}_{KL}(q \| p)$  denotes the Kullback-Leibler (KL) divergence between  $q$  and  $p$ . The first term in the right-hand side of (5) evaluates the reconstruction quality of the decoder, and the second one is a regularization term encouraging the variational posterior to remain close to the prior. As the expectation in (5) is computationally intractable, it is usually approximated by a single sample drawn from  $q(\mathbf{z}|\mathbf{s}; \phi_a)$  [22]. Employing a so-called re-parameterization trick, the set of parameters  $\{\boldsymbol{\theta}, \phi_a\}$  is estimated by a stochastic gradient ascent algorithm [22]. Since all the parameters are inferred using only audio data, the above model is called A-VAE [26]. The associated architecture is shown in Fig. 1 (top).

### B. Visual-only VAE

A visual VAE (V-VAE) is proposed in [26], assuming the same generative model as in (1) and (2). The difference with the A-VAE is that, here, the posterior  $p(\mathbf{z}_n|\mathbf{s}_n)$  is approximated using visual-data only:

$$q(\mathbf{z}_n|\mathbf{v}_n; \phi_v) = \mathcal{N}\left(\boldsymbol{\mu}_z^v(\mathbf{v}_n), \text{diag}\left(\boldsymbol{\sigma}_z^v(\mathbf{v}_n)\right)\right), \quad (6)$$

where,  $\mathbf{v}_n \in \mathbb{R}^M$  is an embedding for the image of the speaker lips at frame  $n$ , and  $\boldsymbol{\mu}_z^v(\cdot) : \mathbb{R}^M \mapsto \mathbb{R}^L$  and  $\boldsymbol{\sigma}_z^v(\cdot) : \mathbb{R}^M \mapsto \mathbb{R}_+^L$  denote neural networks with parameters  $\phi_v$ . Hence, V-VAE attempts to reconstruct clean speech using latent variables inferred from the lips images. The set of parameters,  $\{\boldsymbol{\theta}, \phi_v\}$ , is estimated in the same way as A-VAE. Figure 1 (middle) depicts the architecture of a V-VAE.

### C. Audio-Visual VAE

An audio-visual VAE, called AV-VAE, is also presented in [26] for speech modeling. The rationale of the AV-VAE is to exploit the complementary between audio and visual modalities. The associated generative model is defined as:

$$\mathbf{s}_n|\mathbf{z}_n, \mathbf{v}_n \sim \mathcal{N}_c\left(\mathbf{0}, \text{diag}\left(\boldsymbol{\sigma}_s^v(\mathbf{z}_n, \mathbf{v}_n)\right)\right), \quad (7)$$

$$\mathbf{z}_n|\mathbf{v}_n \sim \mathcal{N}\left(\boldsymbol{\mu}_z^{av}(\mathbf{v}_n), \text{diag}\left(\boldsymbol{\sigma}_z^{av}(\mathbf{v}_n)\right)\right), \quad (8)$$

where,  $\boldsymbol{\sigma}_s^v(\cdot, \cdot) : \mathbb{R}^L \times \mathbb{R}^M \mapsto \mathbb{R}_+^L$  is a neural network taking  $(\mathbf{z}_n, \mathbf{v}_n)$  as input. Furthermore,  $\boldsymbol{\mu}_z^{av}(\cdot) : \mathbb{R}^M \mapsto \mathbb{R}^L$  and  $\boldsymbol{\sigma}_z^{av}(\cdot) : \mathbb{R}^M \mapsto \mathbb{R}_+^L$  are neural networks parameterizing the mean and variance of the prior distribution of  $\mathbf{z}_n$  using  $\mathbf{v}_n$  as the input. The variational approximation to  $p(\mathbf{z}_n|\mathbf{s}_n, \mathbf{v}_n)$  takes a similar form as (3), except that  $\mathbf{v}_n$  is also fed to the associated neural network. The architecture of an AV-VAE is shown in Fig. 1 (bottom).

### III. THE MIXTURE OF INFERENCE NETWORKS VAE

In this section, we aim to devise a framework able to choose the best combination between the auditory and visual encodings, as opposed to systematically using both encodings like in AV-VAE. To achieve this goal, we propose a probabilistic mixture of the audio and visual encoders, and name it mixture of inference networks VAE (MIN-VAE). In a nutshell, the model learns to select if the posterior of  $\mathbf{z}_n$  should be audio- or video-based. The overall architecture is depicted in Fig. 2. In the following we introduce the mathematical formulation associated with the proposed MIN-VAE.

#### A. The Generative Model

We assume that each latent code is generated either from an audio or from a video prior. We model this with a mixing variable  $\alpha_n \in \{0, 1\}$  describing whether the latent code  $\mathbf{z}_n$  corresponds to the audio or to the visual prior. Once the latent code is generated from the corresponding prior, the speech frame  $\mathbf{s}_n$  follows a complex Gaussian with the variance computed by the decoder. We recall that the variance is a non-linear transformation of the latent code.

Formally, each STFT time frame  $\mathbf{s}_n$  is modeled as:

$$\mathbf{s}_n | \mathbf{z}_n, \mathbf{v}_n \sim \mathcal{N}_c \left( \mathbf{0}, \text{diag} \left( \boldsymbol{\sigma}_s(\mathbf{z}_n, \mathbf{v}_n) \right) \right), \quad (9)$$

$$\mathbf{z}_n | \alpha_n \sim \left[ \mathcal{N}(\boldsymbol{\mu}_a, \sigma_a \mathbf{I}) \right]^{\alpha_n} \cdot \left[ \mathcal{N}(\boldsymbol{\mu}_v, \sigma_v \mathbf{I}) \right]^{1-\alpha_n}, \quad (10)$$

$$\alpha_n \sim \pi^{\alpha_n} \times (1 - \pi)^{1-\alpha_n}, \quad (11)$$

where the audio and video priors are parametrized by  $(\boldsymbol{\mu}_a, \sigma_a)$  and  $(\boldsymbol{\mu}_v, \sigma_v)$  respectively, and  $\alpha_n$  is assumed to follow a Bernoulli distribution with parameter  $\pi$ . We propose two versions of this architecture, namely: MIN-VAE-v1 where the decoder (9) takes the same form as (7) and uses explicitly visual information (see Fig. 2), and MIN-VAE-v2 where the decoder (9) takes the same form as (1) and does not use explicitly visual information. In both cases the parameters of the decoder are denoted by  $\boldsymbol{\theta}$ . The derivations will be done for the general case, that is MIN-VAE-v1.

#### B. The Posterior Distribution

In order to estimate the parameters of the generative model described above, i.e.  $\boldsymbol{\psi} = \{\boldsymbol{\mu}_a, \boldsymbol{\mu}_v, \sigma_a, \sigma_v\}$ ,  $\boldsymbol{\theta}$ , and  $\pi$ , we follow a maximum likelihood procedure. To derive it, we need to compute the posterior of the latent variables:

$$p(\mathbf{z}_n, \alpha_n | \mathbf{s}_n, \mathbf{v}_n) = p(\mathbf{z}_n | \mathbf{s}_n, \mathbf{v}_n, \alpha_n) \cdot p(\alpha_n | \mathbf{s}_n, \mathbf{v}_n). \quad (12)$$

The individual factors in the right-hand side of the above equation cannot be computed in closed-form, due to the non-linear generative model. As similarly done in VAE, we pursue an amortized inference approach to approximate  $p(\mathbf{z}_n | \mathbf{s}_n, \mathbf{v}_n, \alpha_n)$  with a parametric Gaussian distribution defined as follows:

$$q(\mathbf{z}_n | \mathbf{s}_n, \mathbf{v}_n, \alpha_n; \boldsymbol{\phi}) = \begin{cases} q(\mathbf{z}_n | \mathbf{s}_n; \boldsymbol{\phi}_a) & \alpha_n = 1, \\ q(\mathbf{z}_n | \mathbf{v}_n; \boldsymbol{\phi}_v) & \alpha_n = 0, \end{cases} \quad (13)$$

in which,  $\boldsymbol{\phi} = \{\boldsymbol{\phi}_a, \boldsymbol{\phi}_v\}$ , and  $\boldsymbol{\phi}_a$  and  $\boldsymbol{\phi}_v$  denote the parameters of the associated audio and visual inference neural

networks, taking the same architectures as those in (3) and (6), respectively. For the posterior of  $\alpha_n$ , i.e.  $p(\alpha_n | \mathbf{s}_n, \mathbf{v}_n)$ , we resort to a variational approximation, denoted  $r(\alpha_n)$ . Put it all together, we have the following approximate posterior:

$$q(\mathbf{z}_n | \mathbf{s}_n, \mathbf{v}_n, \alpha_n; \boldsymbol{\phi}) \cdot r(\alpha_n) \approx p(\mathbf{z}_n, \alpha_n | \mathbf{s}_n, \mathbf{v}_n). \quad (14)$$

#### C. Training the MIN-VAE

In order to train the MIN-VAE, we devise an optimization procedure alternating between estimating  $\boldsymbol{\Theta} = \{\boldsymbol{\phi}, \boldsymbol{\theta}, \boldsymbol{\psi}, \pi\}$  and updating the variational posterior  $r$ . We recall the definition  $\mathbf{s} = \{\mathbf{s}_n\}_{n=1}^{N_{tr}}$ , and  $\mathbf{z}$ , and define  $\boldsymbol{\alpha}$  and  $\mathbf{v}$  analogously. The full posterior of the latent variables can be written as:

$$\begin{aligned} p(\mathbf{z}, \boldsymbol{\alpha} | \mathbf{s}, \mathbf{v}) &= \frac{p(\mathbf{s}, \mathbf{v}, \mathbf{z}, \boldsymbol{\alpha})}{p(\mathbf{s}, \mathbf{v})} \\ &= \frac{p(\mathbf{s} | \mathbf{z}, \mathbf{v}; \boldsymbol{\theta}) p(\mathbf{z} | \boldsymbol{\alpha}) p(\boldsymbol{\alpha})}{p(\mathbf{s}, \mathbf{v}; \boldsymbol{\theta})}. \end{aligned} \quad (15)$$

We then target the KL-divergence between the approximate posterior and the true posterior which reads:

$$\begin{aligned} \mathcal{D}_{KL} \left( q(\mathbf{z} | \mathbf{s}, \mathbf{v}, \boldsymbol{\alpha}; \boldsymbol{\phi}) r(\boldsymbol{\alpha}) \parallel p(\mathbf{z}, \boldsymbol{\alpha} | \mathbf{s}, \mathbf{v}) \right) &= \\ \int_{\mathbb{Z}, \mathbb{A}} q(\mathbf{z} | \mathbf{s}, \mathbf{v}, \boldsymbol{\alpha}; \boldsymbol{\phi}) r(\boldsymbol{\alpha}) \log \frac{q(\mathbf{z} | \mathbf{s}, \mathbf{v}, \boldsymbol{\alpha}; \boldsymbol{\phi}) r(\boldsymbol{\alpha}) p(\mathbf{s}, \mathbf{v}; \boldsymbol{\theta})}{p(\mathbf{s} | \mathbf{z}, \mathbf{v}; \boldsymbol{\theta}) p(\mathbf{z} | \boldsymbol{\alpha}) p(\boldsymbol{\alpha})} d\mathbf{z} d\boldsymbol{\alpha} &= \\ = -\mathcal{L}(\boldsymbol{\Theta}, r) + \log p(\mathbf{s}, \mathbf{v}; \boldsymbol{\theta}) \geq 0, & \quad (16) \end{aligned}$$

where

$$\begin{aligned} \mathcal{L}(\boldsymbol{\Theta}, r) &= \\ \int_{\mathbb{Z}, \mathbb{A}} q(\mathbf{z} | \mathbf{s}, \mathbf{v}, \boldsymbol{\alpha}; \boldsymbol{\phi}) r(\boldsymbol{\alpha}) \log \frac{p(\mathbf{s} | \mathbf{z}, \mathbf{v}; \boldsymbol{\theta}) p(\mathbf{z} | \boldsymbol{\alpha}) p(\boldsymbol{\alpha})}{q(\mathbf{z} | \mathbf{s}, \mathbf{v}, \boldsymbol{\alpha}; \boldsymbol{\phi}) r(\boldsymbol{\alpha})} d\mathbf{z} d\boldsymbol{\alpha}. & \quad (17) \end{aligned}$$

From (16) we can see that  $\log p(\mathbf{s}, \mathbf{v}; \boldsymbol{\theta}) \geq \mathcal{L}(\boldsymbol{\Theta}, r)$ . Therefore, instead of maximizing the intractable data log-likelihood  $\log p(\mathbf{s}, \mathbf{v}; \boldsymbol{\theta})$ , we maximize its lower-bound, i.e.  $\mathcal{L}(\boldsymbol{\Theta}, r)$ , or equivalently:

$$\boldsymbol{\Theta}^*, r^* = \underset{\boldsymbol{\Theta}, r}{\text{argmin}} -\mathcal{L}(\boldsymbol{\Theta}, r) \quad (18)$$

subject to the constraint that  $r$  integrates to one. We solve this problem by alternately optimizing the cost over  $r$  and  $\boldsymbol{\Theta}$ . In the following, the two optimization steps are discussed.

1) *Optimizing w.r.t.  $r(\boldsymbol{\alpha})$* : With  $\boldsymbol{\Theta}$  being fixed to its current estimate, solving (18) boils down to:

$$\min_{r_n(\alpha_n)} \int_{\mathbb{A}} r_n(\alpha_n) \left[ \log \frac{r_n(\alpha_n)}{p(\alpha_n)} + J_n(\alpha_n) \right] d\alpha_n, \forall n, \quad (19)$$

meaning that the optimal  $r$  is separable on  $n$ , where,

$$\begin{aligned} J_n(\alpha_n) &= \\ \int_{\mathbb{Z}} q(\mathbf{z}_n | \mathbf{s}_n, \mathbf{v}_n, \alpha_n; \boldsymbol{\phi}) \log \frac{q(\mathbf{z}_n | \mathbf{s}_n, \mathbf{v}_n, \alpha_n; \boldsymbol{\phi})}{p(\mathbf{s}_n | \mathbf{z}_n, \mathbf{v}_n; \boldsymbol{\theta}) p(\mathbf{z}_n | \alpha_n)} d\mathbf{z}_n &= \\ \mathcal{D}_{KL} \left( q(\mathbf{z}_n | \mathbf{s}_n, \mathbf{v}_n, \alpha_n; \boldsymbol{\phi}) \parallel p(\mathbf{z}_n | \alpha_n) \right) - & \\ \mathbb{E}_{q(\mathbf{z}_n | \mathbf{s}_n, \mathbf{v}_n, \alpha_n; \boldsymbol{\phi})} \left[ \log p(\mathbf{s}_n | \mathbf{z}_n, \mathbf{v}_n; \boldsymbol{\theta}) \right]. & \quad (20) \end{aligned}$$

Using calculus of variations, we find that  $r_n(\alpha_n) \propto p(\alpha_n) \exp(-J_n(\alpha_n))$ , which is a Bernoulli distribution. To

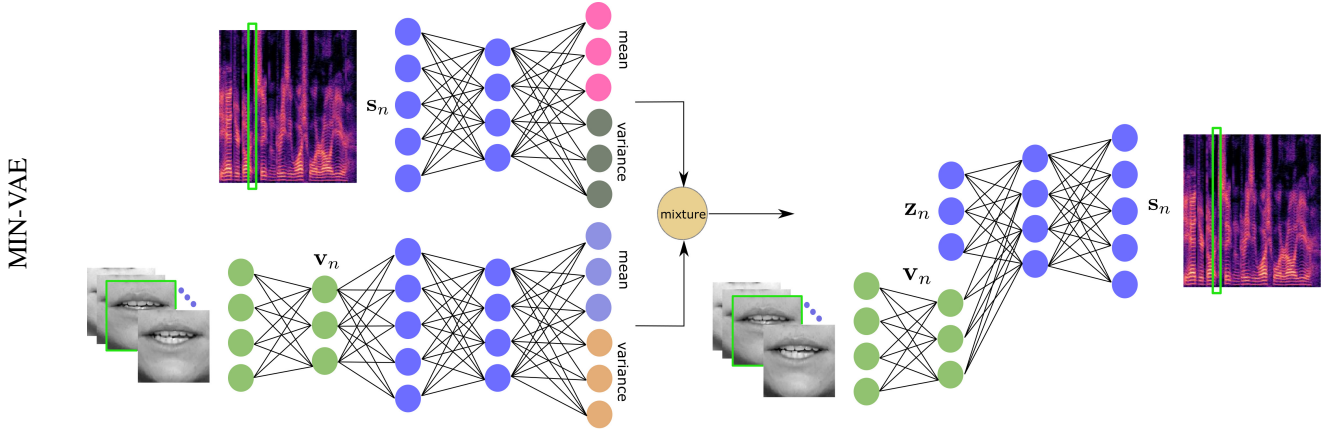


Fig. 2: Architecture of the proposed mixture of inference networks VAE (MIN-VAE). A mixture of an audio- and a video-based encoder is used to approximate the intractable posterior distribution of the latent variables.

find the associated parameter, we need to compute  $J_n(\alpha_n)$ . Since the expectation involved in (20) is intractable to compute, we approximate it using a single sample denoted  $\mathbf{z}_n^{\alpha_n}$  drawn from  $q(\mathbf{z}_n|\mathbf{s}_n, \mathbf{v}_n, \alpha_n; \phi)$ , obtaining:

$$\begin{aligned} \tilde{J}_n(\alpha_n) = \\ \mathcal{D}_{KL}\left(q(\mathbf{z}_n|\mathbf{s}_n, \mathbf{v}_n, \alpha_n; \phi) \parallel p(\mathbf{z}_n|\alpha_n)\right) - \log p(\mathbf{s}_n|\mathbf{z}_n^{\alpha_n}, \mathbf{v}_n; \theta), \end{aligned} \quad (21)$$

The parameter of the Bernoulli distribution then takes the following form:

$$\pi_n = g\left(\tilde{J}_n(\alpha_n = 0) - \tilde{J}_n(\alpha_n = 1) + \log \frac{\pi}{1 - \pi}\right), \quad (22)$$

where  $g(x) = 1/(1 + \exp(-x))$  is the sigmoid function. To compute the KL divergence terms, we use the following lemma:

**Lemma 1.** Let  $p_1(\mathbf{x}; \boldsymbol{\mu}_1, \boldsymbol{\Sigma}_1)$  and  $p_2(\mathbf{x}; \boldsymbol{\mu}_2, \boldsymbol{\Sigma}_2)$  be two multivariate Gaussian distributions in  $\mathbb{R}^n$ . Then, the KL divergence between  $p_1$  and  $p_2$  reads:

$$\begin{aligned} \mathcal{D}_{KL}(p_1 \parallel p_2) = \frac{1}{2} \left( \log \frac{\det \boldsymbol{\Sigma}_2}{\det \boldsymbol{\Sigma}_1} - n + \text{tr}(\boldsymbol{\Sigma}_2^{-1} \boldsymbol{\Sigma}_1) + \right. \\ \left. (\boldsymbol{\mu}_2 - \boldsymbol{\mu}_1)^T \boldsymbol{\Sigma}_2^{-1} (\boldsymbol{\mu}_2 - \boldsymbol{\mu}_1) \right). \end{aligned} \quad (23)$$

Utilizing the above lemma, we can write (for  $\alpha_n = 1$ ):

$$\begin{aligned} \mathcal{D}_{KL}\left(q(\mathbf{z}_n|\mathbf{s}_n; \phi_a) \parallel p(\mathbf{z}_n|\alpha_n)\right) = \frac{1}{2} \log \frac{\sigma_a^L}{\left| \text{diag}(\boldsymbol{\sigma}_z^a(\mathbf{s}_n)) \right|} - \\ + \frac{\text{trace}\left(\text{diag}(\boldsymbol{\sigma}_z^a(\mathbf{s}_n))\right) + \|\boldsymbol{\mu}_z^a(\mathbf{s}_n) - \boldsymbol{\mu}_a\|^2}{2\sigma_a} - \frac{L}{2}, \end{aligned} \quad (24)$$

and analogously for the vision-based term ( $\alpha_n = 0$ ).

2) *Optimizing w.r.t.  $\Theta$ :* With  $r$  being fixed to its current estimate, from (18), we can write the optimization over  $\Theta$  as:

$$\begin{aligned} \min_{\Theta} \int_{\mathbb{Z}, \mathbb{A}} q(\mathbf{z}|\mathbf{s}, \mathbf{v}, \boldsymbol{\alpha}; \phi) r(\boldsymbol{\alpha}) \log \frac{q(\mathbf{z}|\mathbf{s}, \mathbf{v}, \boldsymbol{\alpha}; \phi) r(\boldsymbol{\alpha})}{p(\mathbf{s}|\mathbf{z}, \mathbf{v}; \theta) p(\mathbf{z}|\boldsymbol{\alpha}) p(\boldsymbol{\alpha})} d\mathbf{z} d\boldsymbol{\alpha} \\ = \min_{\Theta} \mathbb{E}_r(\boldsymbol{\alpha}) \left[ \int_{\mathbb{Z}} q(\mathbf{z}|\mathbf{s}, \mathbf{v}, \boldsymbol{\alpha}; \phi) \log \frac{q(\mathbf{z}|\mathbf{s}, \mathbf{v}, \boldsymbol{\alpha}; \phi)}{p(\mathbf{s}|\mathbf{z}, \mathbf{v}; \theta) p(\mathbf{z}|\boldsymbol{\alpha})} d\mathbf{z} \right] \\ + \mathcal{D}_{KL}\left(r(\boldsymbol{\alpha}) \parallel p(\boldsymbol{\alpha})\right) \\ = \min_{\Theta} \sum_{n=0}^{N_{tr}} \mathbb{E}_{r(\alpha_n)} \left[ J_n(\alpha_n) \right] + \mathcal{D}_{KL}\left(r(\alpha_n) \parallel p(\alpha_n)\right) \\ = \min_{\Theta} \sum_{n=0}^{N_{tr}} \pi_n \left( \mathcal{D}_{KL}\left(q(\mathbf{z}_n|\mathbf{s}_n; \phi_a) \parallel p(\mathbf{z}_n|\alpha_n = 1)\right) - \right. \\ \left. \mathbb{E}_{q(\mathbf{z}_n|\mathbf{s}_n; \phi_a)} \left[ \log p(\mathbf{s}_n|\mathbf{z}_n, \mathbf{v}_n; \theta) \right] \right) + \\ (1 - \pi_n) \left( \mathcal{D}_{KL}\left(q(\mathbf{z}_n|\mathbf{v}_n; \phi_v) \parallel p(\mathbf{z}_n|\alpha_n = 0)\right) - \right. \\ \left. \mathbb{E}_{q(\mathbf{z}_n|\mathbf{v}_n; \phi_v)} \left[ \log p(\mathbf{s}_n|\mathbf{z}_n, \mathbf{v}_n; \theta) \right] \right) + \mathcal{D}_{KL}\left(r(\alpha_n) \parallel p(\alpha_n)\right). \end{aligned} \quad (25)$$

As before, the expectations involved in the above equation are approximated with a single sample drawn from the associated posteriors, resulting in:

$$\begin{aligned} \sum_{n=1}^{N_{tr}} -\pi_n \ln p(\mathbf{s}_n|\mathbf{z}_n^a; \theta) - (1 - \pi_n) \ln p(\mathbf{s}_n|\mathbf{z}_n^v; \theta) + \\ \pi_n \mathcal{D}_{KL}\left(q(\mathbf{z}_n|\mathbf{s}_n; \phi_a) \parallel p(\mathbf{z}_n|\alpha_n = 1)\right) + \mathcal{D}_{KL}\left(r(\alpha_n) \parallel p(\alpha_n)\right) \\ + (1 - \pi_n) \mathcal{D}_{KL}\left(q(\mathbf{z}_n|\mathbf{v}_n; \phi_v) \parallel p(\mathbf{z}_n|\alpha_n = 0)\right), \end{aligned} \quad (26)$$

where,  $\mathbf{z}_n^a \sim q(\mathbf{z}_n|\mathbf{s}_n; \phi_a)$  and  $\mathbf{z}_n^v \sim q(\mathbf{z}_n|\mathbf{v}_n; \phi_v)$ . After computing the cost function, the parameters are updated using a reparametrization trick along with a stochastic gradient descent algorithm, e.g. the Adam optimizer. Finally, optimizing (26) over  $\pi$  leads to minimizing the following KL-divergence:

$$\mathcal{D}_{KL}\left(q(\alpha_n) \parallel p(\alpha_n)\right) = \pi_n \log \frac{\pi_n}{\pi} + (1 - \pi_n) \log \frac{1 - \pi_n}{\pi}, \quad (27)$$

yielding

$$\pi = \frac{1}{N_{tr}} \sum_{n=1}^{N_{tr}} \pi_n. \quad (28)$$

Now, with the derived variational inference formulas, we obtain the inference mixture for the MIN-VAE:

$$p(\mathbf{z}_n | \mathbf{s}_n, \mathbf{v}_n) = \pi_n \mathcal{N}(\boldsymbol{\mu}_z^a(\mathbf{s}_n), \text{diag}(\boldsymbol{\sigma}_z^a(\mathbf{s}_n))) \quad (29)$$

$$+ (1 - \pi_n) \mathcal{N}(\boldsymbol{\mu}_z^v(\mathbf{v}_n), \text{diag}(\boldsymbol{\sigma}_z^v(\mathbf{v}_n))). \quad (30)$$

The overall training algorithm then consists of alternating the variational distribution update of  $\alpha_n$  via (22), the update of  $\phi$ ,  $\theta$ , and  $\psi$  via stochastic gradient descent of (26), and the update of  $\pi$  using (28).

#### D. Noise Modeling

At test time, once the MIN-VAE is trained, the STFT time frames of the observed noisy speech are modeled as  $\mathbf{x}_n = \mathbf{s}_n + \mathbf{b}_n$ , for  $n = 0, \dots, N - 1$ , with  $\mathbf{b}_n$  denoting noise STFT time frame. For the probabilistic modeling of  $\mathbf{s}_n$ , we use the generative model trained on clean data (i.e. the previous section). For  $\mathbf{b}_n$ , the following NMF based model is considered [16]:

$$\mathbf{b}_n \sim \mathcal{N}(\mathbf{0}, \text{diag}(\mathbf{W}\mathbf{h}_n)), \quad (31)$$

where,  $\mathbf{W} \in \mathbb{R}_+^{F \times K}$ , and  $\mathbf{h}_n$  denotes the  $n$ -th column of  $\mathbf{H} \in \mathbb{R}_+^{K \times N}$ . The parameters, i.e.  $\{\mathbf{W}, \mathbf{H}\}$ , as well as the unknown speech are then estimated following a Monte-Carlo Expectation-Maximization (MCEM) method [28]. This strategy is inspired by the recent literature [16], [27]. The details are provided in Appendix A.

## IV. EXPERIMENTS

In this section, we aim to evaluate the speech enhancement performance of different VAE architectures, including A-VAE [16], V-VAE [26], AV-VAE [26], and the proposed MIN-VAE. We consider two versions of our proposed network. The first one, named MIN-VAE-v1, is shown in Fig. 2. The second version, referred to as MIN-VAE-v2, shares the same architecture as MIN-VAE-v1 except that the visual features are not used in the decoder. To measure the performance, we use standard scores, including the signal-to-distortion ratio (SDR) [29], the perceptual evaluation of speech quality (PESQ) [30], and the short-time objective intelligibility (STOI) [31]. SDR is measured in decibel (dB), while PESQ and STOI values lie in the intervals  $[-0.5, 4.5]$  and  $[0, 1]$ , respectively (the higher the better). For each measure, we report the averaged difference between the output value (evaluated on the enhanced speech signal) and the input value (evaluated on the noisy/unprocessed mixture signal).

#### A. Experimental Set-up

*a) Dataset:* We use the NTCD-TIMIT dataset [32], which contains audio-visual (AV) recordings from 56 English speakers with an Irish accent, uttering 5488 different TIMIT sentences [33]. The visual data consists of 30 FPS videos of

lips region of interests (ROIs). Each frame (ROI) is of size  $67 \times 67$  pixels. The speech signal is sampled at 16 kHz, and the audio spectral features are computed using an STFT window of 64 ms (1024 samples per frame) with 47.9% overlap, hence  $F = 513$ . The dataset is divided into 39 speakers for training, 8 speakers for validation, and 9 speakers for testing, as proposed in [32]. The test set includes about 1 hour noisy speech, along with their corresponding lips ROIs, with six different noise types, including *Living Room (LR)*, *White*, *Cafe*, *Car*, *Babble*, and *Street*, with noise levels:  $\{-15, -10, -5, 0, 5, 10, 15\}$  dB.

*b) Architecture and training details:* The generative networks (decoders) of A-VAE and V-VAE consist of a single hidden layer with 128 nodes and hyperbolic tangent activations. The dimension of the latent space is  $L = 32$ . The A-VAE encoder has a single hidden layer with 128 nodes and hyperbolic tangent activations. The V-VAE encoder is similar to that, except for extracting visual features embedding lip ROIs into a feature vector  $\mathbf{v}_n \in \mathbb{R}^M$ , with  $M = 128$ . This is composed of two fully-connected layers with 512 and 128 nodes, respectively. The dimension of the input corresponds to a single vectorized frame, namely  $4489 = 67 \times 67$ . AV-VAE combines the architectures of A-VAE and V-VAE as illustrated in Fig. 1. The audio and the video encoders in Fig. 2 share also the same architectures as those of A-VAE and V-VAE encoders, respectively.

To have a fair comparison, we fine-tuned the A-VAE and V-VAE of [26], which have been trained with a standard Gaussian prior for the latent variables, by using a parametric Gaussian prior, as the ones in (10). The decoder parameters of MIN-VAE-v1 and MIN-VAE-v2 are initialized with those of the pretrained AV-VAE and A-VAE, respectively. The parameters of the audio and the video encoders are also initialized with the corresponding parameters in the pretrained A-VAE and V-VAE encoders. Then, all the parameters are fine-tuned using the Adam optimizer [34] with a step size of  $10^{-4}$ , for 100 epochs, and with a batch-size of 128.

We also considered another way to combine A-VAE with V-VAE, in which these two VAE architectures share the same decoder, and they are trained alternately. That is, at each epoch, the shared decoder is trained using latent samples coming from either the encoder of A-VAE or that of V-VAE. As a result, at each epoch, only the encoder parameters of the corresponding VAE are updated while those of the other encoder are kept fixed. We refer to the resulting VAE as A\V-VAE. A description of all the proposed VAE architectures is given in Table I.

TABLE I: Description of the proposed VAE networks.

Name	Description
MIN-VAE-v1	The architecture shown in Fig. 2.
MIN-VAE-v2	Same as MIN-VAE-v1 but without using visual modality in the decoder.
A\V-VAE	Alternately training an A-VAE and a V-VAE with a shared decoder.

*c) Speech enhancement parameters:* For all the methods, the rank of  $\mathbf{W}$  and  $\mathbf{H}$  in the noise model (31) is set to  $K = 10$ ,

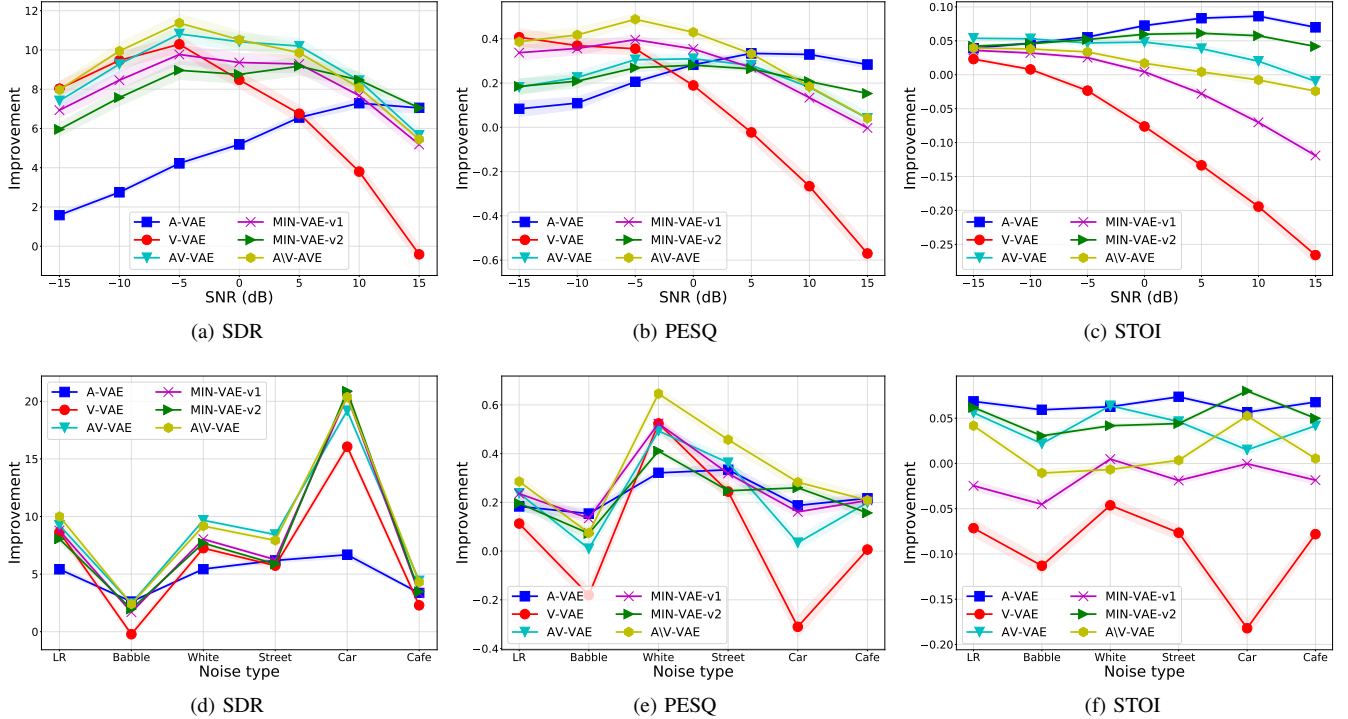


Fig. 3: Performance comparison of different VAE architectures for speech enhancement. Top row shows the averaged results in terms of input noise levels, whereas the bottom row reports the averaged results versus different noise types. Here, no noise was added to the input of the audio-encoders of MIN-VAE-v1 and MIN-VAE-v2 during training.

and these matrices are randomly initialized with non-negative entries. At the first iteration of the inference algorithms, the Markov chain of the Metropolis-Hastings algorithm (see Section A-A2) is initialized by using the noisy observed speech and the visual features as input to the associated encoders, and taking the posterior mean as the initialization of the latent codes. For the proposed VAE architectures, i.e. MIN-VAE-v1, MIN-VAE-v2, and A\VAE, the visual-encoders were used.

## B. Results and Discussion

Figure 3 summarizes the results of all the VAE architectures, in terms of SDR, PESQ, and STOI. The top row of this figure reports the averaged results versus different noise levels, whereas the bottom row shows the averaged results in terms of noise type. From this figure we can see that V-VAE performs pretty well at high noise levels. However, the intelligibility improvements in terms of STOI are not as good as those of the other algorithms. A\VAE, on the other hand, outperforms other methods in terms of SDR and PESQ at high noise levels. Nevertheless, its intelligibility improvements are not satisfactory. The proposed MIN-VAE methods also outperform A-VAE, especially at high noise levels. As explained earlier, this might be due to the facts that the proposed networks efficiently make use of the robust initialization provided by the visual data, and also by the richer generative models (decoders) which are trained using both audio and visual latent codes. At high noise levels, MIN-VAE-v1 outperforms MIN-VAE-v2, implying the importance of using visual modality in the decoder when the input speech is very noisy. A related

observation is that, MIN-VAE-v2 outperforms both MIN-VAE-v1 and AV-VAE when the level of noise is low, implying that the visual features in the generative model contribute mainly in high noise regimes. Part of the worse performance of AV-VAE could be explained by the way the latent codes are initialized, which is based on concatenation of noisy audio and clean visual data. It is worth mentioning that in the low noise regime, the amount of performance improvement is decreasing for all the methods. In fact, it is difficult to enhance a less noisy speech signal.

Regarding noise type, we can see that the algorithms perform very differently. The *Babble* noise is the most difficult noise environment according to the bottom row of Fig. 3. In terms of SDR, all the methods show their best performance for the *Car* noise, with a very large improvement achieved by the audio-visual based methods. In terms of PESQ, the *White* noise is the easiest one for all the methods, especially A\VAE that shows the best performance. Finally, in terms of STOI, MIN-VAE-v2 achieves the best performance for the *Car* noise.

To encourage the proposed MIN-VAE networks to make use of the visual data in the encoder more efficiently, we added some uniform noise to about one-third of speech spectrogram time frames that are fed to the audio encoder of the proposed VAE architectures. Figure 4 presents the results of this experiment. A clear performance improvement is observed compared to Fig. 3, especially for ME-AVE-v2. With this new training, the proposed algorithms outperform AV-VAE in all noise levels. The SDR improvements for high noise levels, however,

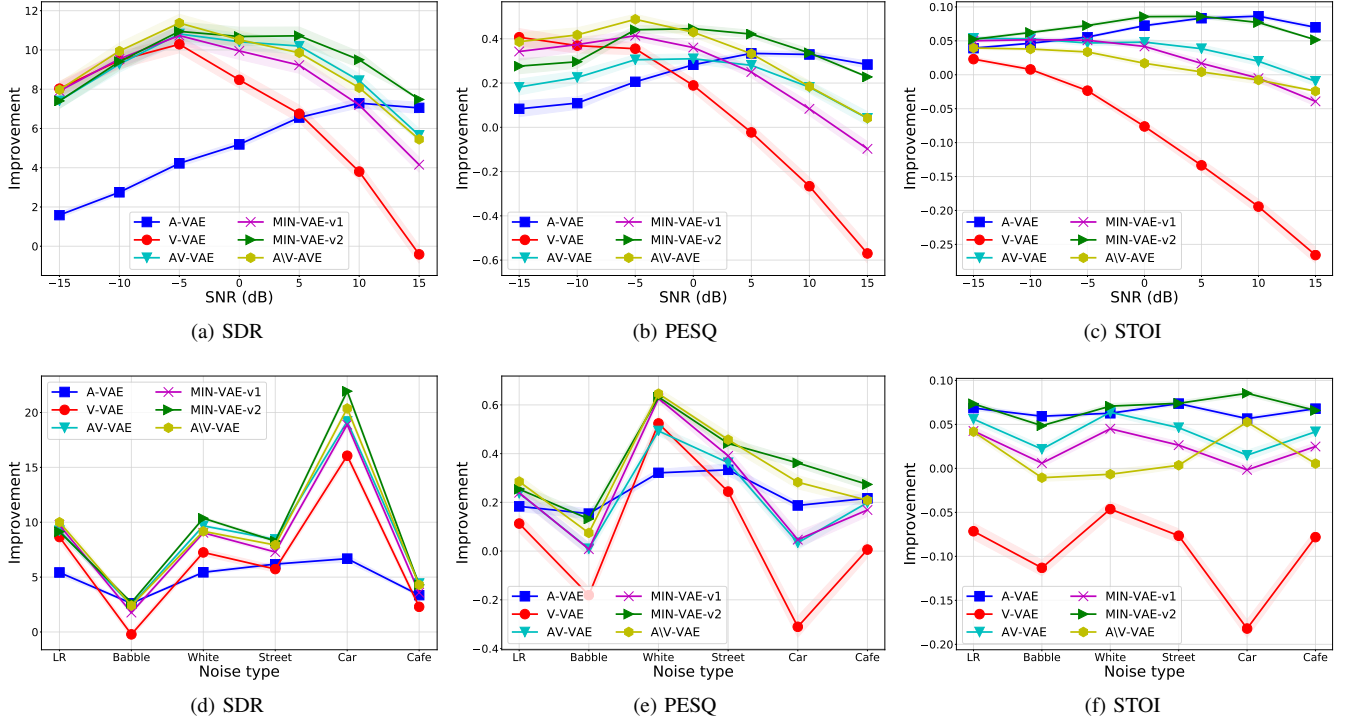


Fig. 4: Performance comparison of different VAE architectures for speech enhancement. Top row shows the averaged results in terms of input noise levels, whereas the bottom row reports the averaged results versus different noise types. Here, some uniform noise was added to the input of the audio-encoders in MIN-VAE-v1 and MIN-VAE-v2 during training.

are very close. As a conclusion, the best performing algorithm turns out to be MIN-VAE-v2, outperforming A\|V-VAE, especially at low levels of noise. Some audio examples are available at <https://team.inria.fr/perception/research/min-vaе-se/>.

## V. CONCLUSIONS

Inspired by the importance of latent variable initialization for VAE-based speech enhancement, and as another way than simple concatenation to effectively fuse audio and visual modalities in the encoder of VAE, we proposed a mixture of inference (audio and visual encoder) networks, which are jointly trained with a shared generative network. The overall architecture is named MIN-VAE. A variational inference approach was proposed to estimate the parameters of the model. At test phase of the speech enhancement, the initialization of the latent variables, as required by the MCEM inference method, is based on the visual modality, which is assumed to be clean in contrast to audio data. As such, it provides a better performance than initializing with noisy audio data. This is confirmed by our experiments, comparing different VAE architectures.

Some future works include making the proposed algorithms robust to noisy visual data, e.g. by using the mixture idea suggested in [27], incorporating the time dependency between audio and visual time frames by utilizing recurrent layers, and reducing the computational complexity of the inference.

## APPENDIX A SPEECH ENHANCEMENT

The generative model consists of (9), (10), and (11), where all the parameters except  $\pi$  have already been trained on clean audio and visual data. The observations are noisy STFT frames  $\mathbf{x} = \{\mathbf{x}_n\}_{n=0}^{N-1}$ , as well as the visual data  $\mathbf{v} = \{\mathbf{v}_n\}_{n=0}^{N-1}$ . The latent variables of the model are  $\mathbf{s} = \{\mathbf{s}_n\}_{n=0}^{N-1}$ ,  $\mathbf{z} = \{\mathbf{z}_n\}_{n=0}^{N-1}$ , and  $\alpha = \{\alpha_n\}_{n=0}^{N-1}$ . Furthermore, the parameters of the model are  $\Theta = \{\mathbf{W}, \mathbf{H}, \pi\}$ .

### A. Parameters Estimation

The full posterior is written as:

$$p(\mathbf{s}_n, \mathbf{z}_n, \alpha_n | \mathbf{x}_n, \mathbf{v}_n; \Theta) \propto p(\mathbf{x}_n, \mathbf{s}_n, \mathbf{z}_n, \mathbf{v}_n, \alpha_n; \Theta) = p(\mathbf{x}_n | \mathbf{s}_n; \Theta) \times p(\mathbf{s}_n | \mathbf{z}_n, \mathbf{v}_n) \times p(\mathbf{z}_n | \alpha_n) \times p(\alpha_n) \quad (32)$$

To estimate the parameter set, we use variational expectation-maximization (VEM) [28], where in the variational expectation step (VE-step), the above intractable posterior is approximated by a variational distribution  $r(\mathbf{s}_n, \mathbf{z}_n, \alpha_n)$ , as similarly done in [27]. The maximization step (M-step) performs parameters update using the obtained variational distributions. We assume that  $r$  factorizes as follows:

$$r(\mathbf{s}_n, \mathbf{z}_n, \alpha_n) = r(\mathbf{s}_n) \times r(\mathbf{z}_n) \times r(\alpha_n). \quad (33)$$

Denoting the current estimate of the parameters as  $\Theta^{old}$ , the VEM approach consists of iterating between the VE-steps and the M-step, which are detailed below.



1) *VE- $r(\mathbf{s}_n)$  step*: The variational distribution of  $\mathbf{s}_n$  is computed as [28]:

$$\begin{aligned} r(\mathbf{s}_n) &\propto \exp\left(\mathbb{E}_{r(\mathbf{z}_n) \cdot r(\alpha_n)}\left[\log p(\mathbf{x}_n, \mathbf{s}_n, \mathbf{z}_n, \alpha_n, \mathbf{v}_n; \Theta^{old})\right]\right) \\ &\propto \exp\left(\mathbb{E}_{r(\mathbf{z}_n)}\left[\log p(\mathbf{x}_n | \mathbf{s}_n; \Theta^{old}) + \log p(\mathbf{s}_n | \mathbf{z}_n, \mathbf{v}_n)\right]\right) \\ &= \exp\left(-\sum_f \left[\frac{|x_{fn} - s_{fn}|^2}{(\mathbf{W}\mathbf{H})_{fn}} + \frac{|s_{fn}|^2}{\gamma_{fn}}\right]\right), \end{aligned} \quad (34)$$

where,

$$\gamma_{fn}^{-1} = \mathbb{E}_{r(\mathbf{z}_n)} \left[ \frac{1}{\sigma_{s,f}(\mathbf{z}_n^{(d)}, \mathbf{v}_n)} \right] \approx \frac{1}{D} \sum_{d=1}^D \frac{1}{\sigma_{s,f}(\mathbf{z}_n^{(d)}, \mathbf{v}_n)}, \quad (35)$$

and  $\{\mathbf{z}_n^{(d)}\}_{d=1}^D$  is a sequence sampled from  $r(\mathbf{z}_n)$ . From (34), we can see that  $r(s_{fn}) = \mathcal{N}_c(m_{fn}, \nu_{fn})$ , where:

$$\begin{cases} m_{fn} &= \frac{\gamma_{fn}}{\gamma_{fn} + (\mathbf{W}\mathbf{H})_{fn}} \cdot x_{fn} \\ \nu_{fn} &= \frac{\gamma_{fn} \cdot (\mathbf{W}\mathbf{H})_{fn}}{\gamma_{fn} + (\mathbf{W}\mathbf{H})_{fn}} \end{cases}. \quad (36)$$

2) *VE- $r(\mathbf{z}_n)$  step*: The variational distribution of  $\mathbf{z}_n$  can be computed by the following standard formula:

$$\begin{aligned} r(\mathbf{z}_n) &\propto \exp\left(\mathbb{E}_{r(\mathbf{s}_n) \cdot r(\alpha_n)}\left[\log p(\mathbf{x}_n, \mathbf{s}_n, \mathbf{z}_n, \alpha_n, \mathbf{v}_n; \Theta^{old})\right]\right) \\ &\propto \exp\left(\mathbb{E}_{r(\mathbf{s}_n) \cdot r(\alpha_n)}\left[\log p(\mathbf{s}_n | \mathbf{z}_n, \mathbf{v}_n) + \log p(\mathbf{z}_n | \alpha_n)\right]\right) \\ &\propto \exp\left(\sum_f -\log\left(\sigma_{s,f}(\mathbf{z}_n, \mathbf{v}_n)\right) - \frac{|m_{fn}|^2 + \nu_{fn}}{\sigma_{s,f}(\mathbf{z}_n, \mathbf{v}_n)}\right) \\ &+ \sum_{\alpha_n \in \{0,1\}} r(\alpha_n) \cdot \left[\log p(\mathbf{z}_n | \alpha_n)\right] \triangleq \tilde{r}(\mathbf{z}_n) \end{aligned} \quad (37)$$

This gives us an unnormalized distribution  $\tilde{r}(\mathbf{z}_n)$  whose normalization constant cannot be computed in closed-form, due to the non-linear terms. However, we use the Metropolis-Hastings algorithm [28] to sample from it. To that end, we need to start with an initialization,  $\mathbf{z}^{(0)}$ . At the beginning of the inference,  $\mathbf{z}^{(0)}$  is set to be the posterior mean in the output of the visual-encoder, i.e. the bottom-left network in Fig. 2, where  $\mathbf{v}_n$  is given as the input. Then, a candidate sample denoted  $\mathbf{z}^{(c)}$  is obtained by sampling from a proposal distribution, usually chosen to be a Gaussian:

$$\mathbf{z}^{(c)} | \mathbf{z}^{(0)} \sim \mathcal{N}(\mathbf{z}^{(0)}, \epsilon \mathbf{I}), \quad (38)$$

where,  $\epsilon > 0$  controls the speed of convergence. Then,  $\mathbf{z}^{(c)}$  is set to be the next sample  $\mathbf{z}^{(1)}$  with the following probability:

$$p = \min\left(1, \frac{\tilde{r}(\mathbf{z}^{(c)})}{\tilde{r}(\mathbf{z}^{(0)})}\right). \quad (39)$$

That means, some  $u$  is drawn from a uniform distribution between 0 and 1. Then, if  $u < p$ , the sample is accepted and  $\mathbf{z}^{(1)} = \mathbf{z}^{(c)}$ . Otherwise, it is rejected and  $\mathbf{z}^{(1)} = \mathbf{z}^{(0)}$ . This procedure is repeated until the required number of samples is achieved. The first few samples are usually discarded, as they are not so reliable.

3) *VE- $r(\alpha_n)$  step*: The variational distribution of  $\alpha_n$  is computed as:

$$\begin{aligned} r(\alpha_n) &\propto \exp\left(\mathbb{E}_{r(\mathbf{s}_n) \cdot r(\mathbf{z}_n)}\left[\log p(\mathbf{x}_n, \mathbf{s}_n, \mathbf{z}_n, \alpha_n, \mathbf{v}_n; \Theta^{old})\right]\right) \\ &\propto p(\alpha_n) \times \exp\left(\mathbb{E}_{r(\mathbf{z}_n)}\left[\alpha_n \cdot \log p(\mathbf{z}_n | \alpha_n = 1) \right. \right. \\ &\quad \left. \left. + (1 - \alpha_n) \cdot \log p(\mathbf{z}_n | \alpha_n = 0)\right]\right) \end{aligned} \quad (40)$$

which is a Bernoulli distribution with the following parameter:

$$\pi_n = g\left(\mathbb{E}_{r(\mathbf{z}_n)}\left[\log \frac{p(\mathbf{z}_n | \alpha_n = 1)}{p(\mathbf{z}_n | \alpha_n = 0)}\right] + \log \frac{\pi}{1 - \pi}\right), \quad (41)$$

with  $g(\cdot)$  being the sigmoid function.

4) *M-step*: After updating all the variational distributions, the next step is to update the set of parameters, i.e.  $\Theta = \{\mathbf{W}, \mathbf{H}, \pi\}$ . To do so, we need to optimize the complete-data log-likelihood which reads:

$$\begin{aligned} Q(\Theta; \Theta^{old}) &= \mathbb{E}_{r(\mathbf{s}) \cdot r(\mathbf{z}) \cdot r(\alpha)}\left[\log p(\mathbf{x}, \mathbf{s}, \mathbf{z}, \alpha, \mathbf{v}; \Theta)\right] \\ &\stackrel{cte.}{=} \mathbb{E}_{r(\mathbf{s})}\left[\log p(\mathbf{x} | \mathbf{s}; \Theta)\right] + \mathbb{E}_{r(\alpha)}\left[\log p(\alpha)\right] \\ &\stackrel{cte.}{=} \sum_{f,n} -\frac{|x_{fn} - m_{fn}|^2 + \nu_{fn}}{(\mathbf{W}\mathbf{H})_{fn}} - \log(\mathbf{W}\mathbf{H})_{fn} \\ &\quad + \pi_n \log \pi + (1 - \pi_n) \log(1 - \pi) \end{aligned} \quad (42)$$

The update formulas for  $\mathbf{W}$  and  $\mathbf{H}$  can be obtained by using standard multiplicative updates [35]:

$$\mathbf{H} \leftarrow \mathbf{H} \odot \frac{\mathbf{W}^\top (\mathbf{V} \odot (\mathbf{W}\mathbf{H})^{\odot -2})}{\mathbf{W}^\top (\mathbf{W}\mathbf{H})^{\odot -1}}, \quad (43)$$

$$\mathbf{W} \leftarrow \mathbf{W} \odot \frac{(\mathbf{V} \odot (\mathbf{W}\mathbf{H})^{\odot -2}) \mathbf{H}^\top}{(\mathbf{W}\mathbf{H})^{\odot -1} \mathbf{H}^\top}, \quad (44)$$

where  $\mathbf{V} = \left[|x_{fn} - m_{fn}|^2 + \nu_{fn}\right]_{(f,n)}$ . Optimizing over  $\pi$  leads to a similar update formula as in (28):

$$\pi = \frac{1}{N} \sum_{n=1}^N \pi_n. \quad (45)$$

## B. Speech Estimation

Let  $\Theta^* = \{\mathbf{W}^*, \mathbf{H}^*, \pi^*\}$  denote the optimal set of parameters found by the above VEM procedure. An estimation of the clean speech is then obtained as the variational posterior mean ( $\forall f, n$ ):

$$\hat{s}_{fn} = \mathbb{E}_{r(s_{fn})}[s_{fn}] = \frac{\gamma_{fn}^*}{\gamma_{fn}^* + (\mathbf{W}^* \mathbf{H}^*)_{fn}} \cdot x_{fn}, \quad (46)$$

where,  $\gamma_{fn}^*$ , defined in (35), is computed using the optimal parameters.

## REFERENCES

- [1] E. Vincent, T. Virtanen, and S. Gannot, *Audio Source Separation and Speech Enhancement*, Wiley, 2018.
- [2] P. C. Loizou, *Speech enhancement: theory and practice*, CRC press, 2007.
- [3] S. Boll, "Suppression of acoustic noise in speech using spectral subtraction," *IEEE Transactions on Acoustics, Speech, and Signal Processing*, vol. 27, no. 2, pp. 113–120, 1979.
- [4] J. S. Lim and A. V. Oppenheim, "Enhancement and bandwidth compression of noisy speech," *Proceedings of the IEEE*, vol. 67, no. 12, pp. 1586–1604, 1979.
- [5] W. DeLiang and J. Chen, "Supervised speech separation based on deep learning: An overview," *IEEE Transactions on Audio, Speech, and Language Processing*, vol. 26, no. 10, pp. 1702–1726, 2018.
- [6] Y. Xu, J. Du, L.-R. Dai, and C.-H. Lee, "A regression approach to speech enhancement based on deep neural networks," *IEEE Transactions on Audio, Speech, and Language Processing*, vol. 23, no. 1, pp. 7–19, 2015.
- [7] X. Li and R. Horaud, "Multichannel speech enhancement based on time-frequency masking using subband long short-term memory," in *IEEE Workshop on Applications of Signal Processing to Audio and Acoustics*, 2019, pp. 1–5.
- [8] K. Wilson, B. Raj, P. Smaragdis, and A. Divakaran, "Speech denoising using nonnegative matrix factorization with priors," in *Proc. IEEE International Conference on Acoustics, Speech and Signal Processing (ICASSP)*, Las Vegas, USA, 2008, pp. 4029–4032.
- [9] Nasser Mohammadiha, Paris Smaragdis, and Arne Leijon, "Supervised and unsupervised speech enhancement using nonnegative matrix factorization," *IEEE Transactions on Audio, Speech, and Language Processing*, vol. 21, no. 10, pp. 2140–2151, 2013.
- [10] F. Sedighin, M. Babaie-Zadeh, B. Rivet, and C. Jutten, "Multimodal soft nonnegative matrix co-factorization for convolutive source separation," vol. 65, no. 12, pp. 3179–3190, 2017.
- [11] C. Févotte, N. Bertin, and J.-L. Durrieu, "Nonnegative matrix factorization with the Itakura-Saito divergence: With application to music analysis," *Neural computation*, vol. 21, no. 3, pp. 793–830, 2009.
- [12] F. Smaragdis, B. Raj, and M. Shashanka, "Supervised and semi-supervised separation of sounds from single-channel mixtures," in *Proc. Int. Conf. Indep. Component Analysis and Signal Separation*, 2007, pp. 414–421.
- [13] G. J. Mysore and P. Smaragdis, "A non-negative approach to semi-supervised separation of speech from noise with the use of temporal dynamics," in *2011 IEEE International Conference on Acoustics, Speech and Signal Processing (ICASSP)*, 2011.
- [14] M. Sun, X. Zhang, and T. F. Zheng, "Unseen noise estimation using separable deep auto encoder for speech enhancement," vol. 24, no. 1, pp. 93–104, 2016.
- [15] Y. Bando, M. Mimura, K. Itoyama, K. Yoshii, and T. Kawahara, "Statistical speech enhancement based on probabilistic integration of variational autoencoder and non-negative matrix factorization," in *Proc. IEEE International Conference on Acoustics, Speech, and Signal Processing (ICASSP)*, 2018, pp. 716–720.
- [16] S. Leglaive, L. Girin, and R. Horaud, "A variance modeling framework based on variational autoencoders for speech enhancement," in *Proc. IEEE International Workshop on Machine Learning for Signal Processing (MLSP)*, 2018, pp. 1–6.
- [17] K. Sekiguchi, Y. Bando, K. Yoshii, and T. Kawahara, "Bayesian multichannel speech enhancement with a deep speech prior," in *Proc. Asia-Pacific Signal and Information Processing Association Annual Summit and Conference (APSIPA ASC)*, 2018, pp. 1233–1239.
- [18] M. Pariente, A. Deleforge, and E. Vincent, "A statistically principled and computationally efficient approach to speech enhancement using variational autoencoders," in *Proc. Conference of the International Speech Communication Association (INTERSPEECH)*, 2019.
- [19] S. Leglaive, U. Şimşekli, A. Liutkus, L. Girin, and R. Horaud, "Speech enhancement with variational autoencoders and alpha-stable distributions," in *Proc. IEEE International Conference on Acoustics, Speech, and Signal Processing (ICASSP)*, 2019, pp. 541–545.
- [20] H. Kameoka, L. Li, S. Inoue, and S. Makino, "Supervised determined source separation with multichannel variational autoencoder," *Neural Computation*, vol. 31, no. 9, pp. 1–24, 2019.
- [21] D. J. Rezende, S. Mohamed, and D. Wierstra, "Stochastic backpropagation and approximate inference in deep generative models," in *Proceedings of the 31st International Conference on Machine Learning (ICML)*, 2014.
- [22] D. P. Kingma and M. Welling, "Auto-encoding variational bayes," in *International Conference on Learning Representations (ICLR)*, 2014.
- [23] L. Girin, J.-L. Schwartz, and G. Feng, "Audio-visual enhancement of speech in noise," *The Journal of the Acoustical Society of America*, vol. 109, no. 6, pp. 3007–3020, 2001.
- [24] T. Afouras, J. S. Chung, and A. Zisserman, "The conversation: Deep audio-visual speech enhancement," in *Proc. Conference of the International Speech Communication Association (INTERSPEECH)*, 2018, pp. 3244–3248.
- [25] A. Gabbay, A. Shamir, and S. Peleg, "Visual speech enhancement," in *Proc. Conference of the International Speech Communication Association (INTERSPEECH)*, 2018, pp. 1170–1174.
- [26] M. Sadeghi, S. Leglaive, X. Alameda-Pineda, L. Girin, and R. Horaud, "Audio-visual speech enhancement using conditional variational autoencoders," *IEEE/ACM Transactions on Audio, Speech and Language Processing*, (to appear) 2020.
- [27] M. Sadeghi and X. Alameda-Pineda, "Robust unsupervised audio-visual speech enhancement using a mixture of variational autoencoders," in *Proc. IEEE International Conference on Acoustics, Speech, and Signal Processing (ICASSP)*, 2020.
- [28] C. Bishop, *Pattern Recognition and Machine Learning*, Springer-Verlag Berlin, Heidelberg, 2006.
- [29] E. Vincent, R. Gribonval, and C. Févotte, "Performance measurement in blind audio source separation," *IEEE Transactions on Audio, Speech, and Language Processing*, vol. 14, no. 4, pp. 1462–1469, 2006.
- [30] A. W. Rix, J. G. Beerends, M. P. Hollier, and A. P. Hekstra, "Perceptual evaluation of speech quality (PESQ)-a new method for speech quality assessment of telephone networks and codecs," in *Proc. IEEE International Conference on Acoustics, Speech, and Signal Processing (ICASSP)*, 2001, pp. 749–752.
- [31] C. H. Taal, R. C. Hendriks, R. Heusdens, and J. Jensen, "An algorithm for intelligibility prediction of time-frequency weighted noisy speech," *IEEE Trans. Audio, Speech, Language Process.*, vol. 19, no. 7, pp. 2125–2136, 2011.
- [32] A.-H. Abdelaziz, "NTCD-TIMIT: A new database and baseline for noise-robust audio-visual speech recognition," in *Proc. Conference of the International Speech Communication Association (INTERSPEECH)*, 2017, pp. 3752–3756.
- [33] M. S. Garofolo, L. F. Lamel, W. M. Fisher, J. G. Fiscus, D. S. Pallett, N. L. Dahlgren, and V. Zue, "TIMIT acoustic phonetic continuous speech corpus," in *Linguistic data consortium*, 1993.
- [34] D. P. Kingma and J. Ba, "Adam: A method for stochastic optimization," in *International Conference on Learning Representations (ICLR)*, 2015.
- [35] C. Févotte, N. Bertin, and J.-L. Durrieu, "Nonnegative matrix factorization with the Itakura-Saito divergence: With application to music analysis," *Neural computation*, vol. 21, no. 3, pp. 793–830, 2009.